Hexagonal photonic-band-gap structures

D. Cassagne, C. Jouanin, and D. Bertho
Université de Montpellier II, Groupe d'Etude des Semiconducteurs, CC074, Place Eugène Bataillon, 34095 Montpellier Cedex 05, France
(Received 7 June 1995; revised manuscript received 19 October 1995)

We investigate a class of two-dimensional hexagonal structures that possess photonic band gaps. This class includes the previously studied triangular structure as a particular case. By symmetry analysis, we obtain a clear insight into the gap opening and we show how the photonic band gaps are affected by the characteristics of materials, according to whether the dielectric constant of the cylinders is larger or smaller than the background one. The photonic band structures present numerous gaps, and we study the evolution of these gaps as functions of the diameter and nature of cylinders. Our results demonstrate the existence of absolute band gaps for many configurations, largest gaps being obtained for triangular and graphite structures.

I. INTRODUCTION

In the last few years, the study of periodic dielectric structure has received considerable interest because it presents the ability to prevent the propagation of electromagnetic waves in a certain frequency range.[1–8] This results from the removal of degeneracies of the free-photon states at the Bragg planes provoked by the periodicity, which produces forbidden frequency gaps—so-called photonic band gaps (PBG's). It is very attractive to describe the propagation of the electromagnetic waves in these artificial materials in the same way as that of the electron waves in natural crystals, in spite of the large difference between the wavelengths. The dispersion relation gives photonic band structures and some concepts, such as impurity states and effective masses, which are very usual for electrons, can be extended to photons. The existence of such PBG's when they overlap with the electronic gaps is particularly promising with regards to the control the spontaneous emission of light, which is essential for the realization of thresholdless and low-noise semiconductor lasers. The search for structures that possess wide PBG's in the frequency range of interest for the applications has motivated a lot of research.[9–11] To prevent the propagation of the waves, whatever its direction is, the gaps opened at different points of the Brillouin zone must overlap as much as possible so as to give large absolute band gaps. Thus, it is desirable that the different gaps are large and centered on neighboring frequencies. Such a condition can be achieved for the Brillouin zone by deviating slightly from the spherical shape. So, theoretical and experimental investigations on PBG's in three dimensions have first concerned the face-centered cubic lattice. Until now, the experimental realizations of these structures exhibit PBG at microwave frequencies because of the limitations in the fabrication of such materials at submicrometer length scales. Recent attempts to increase the frequency of the gaps have led to the use of more sophisticated structure designs with lower symmetry lattices.[12,13] However, the feasibility of such three-dimensional (3D) structures with the idea of using them in optoelectronic devices is still an important challenge and a way in which to obtain photonic crystals with gaps situated in the infrared is to fabricate 2D crystals consisting of parallel dielectric rods arranged on 2D lattices. As the PBG's yielded by these structures only suppress the propagation of the electromagnetic waves in the lattice plane, the inhibition of the propagation in the third direction can be obtained by inserting the crystal between two Bragg mirrors. For in-plane propagation, two types of electromagnetic modes exist according to whether the electric (E polarization) or magnetic (H polarization) field is parallel to the rod axis. The band gaps occurring in each case must overlap to form an absolute band gap that prevents the propagation of the light of any polarization. Among the 2D Bravais lattices, the hexagonal one possesses the Brillouin zone with the most circular shape, and it is now a well accepted fact that the crystal patterns deduced from it are good candidates to produce large absolute band gaps. Among the systems recently investigated, the triangular structure of air cylinders in GaAs was found to possess large PBG's for a large volume fraction of air.[14–16] Studies depending on the cylinder shape have shown that the largest absolute band gaps are achieved for circular cross sections[17] that are also the most convenient to realize. If the feasibility of such 2D photonic crystals is at that time well demonstrated at the submicrometer lengths,[18–20] no attempt exists to optimize the design of these structures by modifying the configuration of the cylinders in the hexagonal unit cell, their cross section being kept circular.

We are concerned in this paper with the simplest pattern, which is obtained from a hexagonal Bravais lattice by introducing two cylinders in the unit cell, and we consider a class of structures consisting of periodic arrays of two kinds of infinitely long parallel cylinders with circular shaped cross sections, embedded in material with a different dielectric constant. In Sec. II, we present the crystal patterns concerned in this work and we give the main lines of the calculation method. Before carrying out detailed calculations, we first proceed in Sec. III to a symmetry analysis in order to get a clear physical insight into the gap opening. We determine the features of the photonic band structures originating from the lattice symmetry and we show how the nature of photonic crystal plays a fundamental role according to whether the structures are constituted by air cylinders in GaAs or by GaAs cylinders in air. In Sec. IV, we study the evolution of the numerous PBG's that appear as functions of the diameters of the two kinds of cylinders. When the diameter of one cylinder is infinitely small, the already widely studied trian-

gular structure is obtained. For two identical cylinders, structures with the same crystal pattern as the graphite one are generated.[21] In this case, we found that two absolute PBG's can be achieved for systems far from the close-packed configuration. This opportunity could allow an easier realization of photonic crystals by avoiding the etching of thin semiconductor layers, which are necessary in the triangular structure.

II. MODEL AND METHOD

To determine the absolute band gaps, we study the propagation of the waves from Maxwell's equations. In inhomogeneous dielectric materials, the magnetic field is

$$\nabla\times[\,\eta(\mathbf{r})\nabla\times\mathbf{H}(\mathbf{r})\,]=\frac{\omega^2}{c^2}\mathbf{H}(\mathbf{r}), \tag{1}$$

where $\eta(\mathbf{r})$ is the inverse of the dielectric constant. Because of the relation $\nabla\cdot\mathbf{H}(\mathbf{r})=0$, $\mathbf{H}(\mathbf{r})$ is transverse. For periodic systems, it can be expressed as a sum of plane waves:[7]

$$\mathbf{H}(\mathbf{r})=\sum_{\mathbf{G}}\sum_{\lambda=1}^{2} h_{\mathbf{G},\lambda}\hat{\mathbf{e}}_\lambda e^{i(\mathbf{k}+\mathbf{G})\cdot\mathbf{r}}, \tag{2}$$

where $\mathbf{k}$ is a wave vector in the Brillouin zone and $\mathbf{G}$ is a 2D reciprocal lattice vector. For each $\mathbf{G}$, $\hat{\mathbf{e}}_1$ and $\hat{\mathbf{e}}_2$ are unit vectors perpendicular to $\mathbf{k}+\mathbf{G}$. So Eq. (1) is expressed as a matrix equation:

$$\sum_{\mathbf{G}',\lambda'} \mathrm{H}^{\lambda,\lambda'}_{\mathbf{G},\mathbf{G}'}h_{\mathbf{G}',\lambda'}=\frac{\omega^2}{c^2}h_{\mathbf{G},\lambda}\,, \tag{3}$$

where

$$\mathrm{H}_{\mathbf{G},\mathbf{G}'}=|\mathbf{k}+\mathbf{G}||\mathbf{k}+\mathbf{G}'|\,\eta(\mathbf{G}-\mathbf{G}')\begin{bmatrix}\hat{\mathbf{e}}_2\cdot\hat{\mathbf{e}}_2' & -\hat{\mathbf{e}}_2\cdot\hat{\mathbf{e}}_1'\\ -\hat{\mathbf{e}}_1\cdot\hat{\mathbf{e}}_2' & \hat{\mathbf{e}}_1\cdot\hat{\mathbf{e}}_1'\end{bmatrix}. \tag{4}$$

$\eta(\mathbf{G})$ is the Fourier transform of the inverse of $\varepsilon(\mathbf{r})$.

We study a periodic array of parallel dielectric cylinders. We assume that these cylinders are in the direction of the z axis. Their intersections with the x-y plane form a two-dimensional periodic dielectric structure. In this case,

$$\eta(\mathbf{G})=\frac{1}{S_{\mathrm{cell}}}\int_{\mathrm{cell}}\eta(\mathbf{r})e^{-i\mathbf{G}\cdot\mathbf{r}}d\mathbf{r}, \tag{5}$$

where S_{cell} is the surface of the primitive cell of the lattice. We investigate the propagation of the electromagnetic waves in the xy plane. $\mathbf{k}+\mathbf{G}$ is in the x-y plane for all $\mathbf{G}$'s, so we can choose all the $\hat{\mathbf{e}}_1$ vectors identical in the z direction and all the $\hat{\mathbf{e}}_2$ in the x-y plane. In this case, $\hat{\mathbf{e}}_2\cdot\hat{\mathbf{e}}_1'=0$ and $\hat{\mathbf{e}}_1\cdot\hat{\mathbf{e}}_2'=0$. Hence, the matrix equation (4) can be separated into two very different equations. This gives rise to two polarizations. In the E polarization case, $\mathbf{E}(\mathbf{r})$ is parallel to the z axis, $\mathbf{H}(\mathbf{r})$ is in the x-y plane, $h_{\mathbf{G},1}=0$ for all $\mathbf{G}$s and we obtain

$$\sum_{\mathbf{G}'}|\mathbf{k}+\mathbf{G}||\mathbf{k}+\mathbf{G}'|\,\eta(\mathbf{G}-\mathbf{G}')h_{\mathbf{G}',2}=\frac{\omega^2}{c^2}h_{\mathbf{G},2}. \tag{6}$$

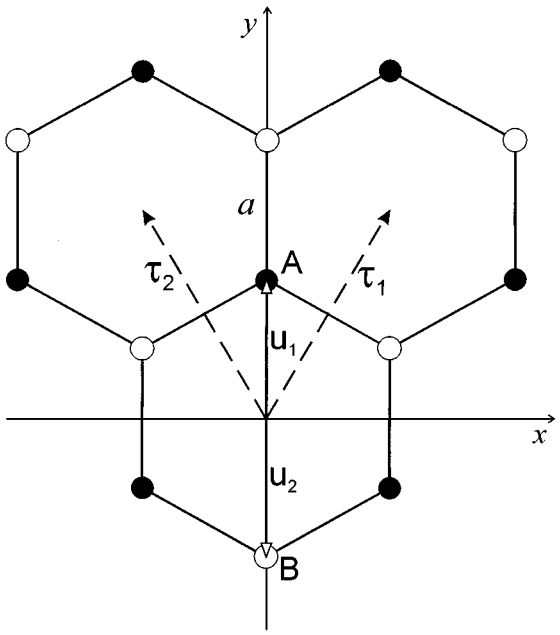

FIG. 1. Two-dimensional triangular, graphite, and boron nitride structures.

For the H polarization, $\mathbf{H}(\mathbf{r})$ is in the z direction, $h_{\mathbf{G},2}=0$ for all $\mathbf{G}$. Seeing that $|\mathbf{k}+\mathbf{G}||\mathbf{k}+\mathbf{G}'|\hat{\mathbf{e}}_2\cdot\hat{\mathbf{e}}_2'=(\mathbf{k}+\mathbf{G})\cdot(\mathbf{k}+\mathbf{G}')$, Eq. (4) gives

$$\sum_{\mathbf{G}'}(\mathbf{k}+\mathbf{G})\cdot(\mathbf{k}+\mathbf{G}')\,\eta(\mathbf{G}-\mathbf{G}')h_{\mathbf{G}',1}=\frac{\omega^2}{c^2}h_{\mathbf{G},1}. \tag{7}$$

These results have been obtained in another way.[14] Consider the 2D periodic structure shown in Fig. 1. This structure allows us to describe the different structures studied in this work by defining two kinds of lattice sites A and B. When all the sites are occupied by identical cylinders, they form a two-dimensional arrangement of hexagons. By analogy with the crystal structure of the graphite, we call this arrangement a graphite structure; it can be considered as being composed of two 2D sublattices made up of identical cylinders. If only the A and B sites are alternatively occupied by cylinders that differ between them by their dimension, or that are made up of different materials, the crystal structure of the boron nitride (BN) is obtained. In this case, the lattice is formed by two sublattices, each one being formed by only one sort of cylinder. Lastly, when only one kind of site is occupied, the triangular structure is found. We limit our study to the structures formed by cylinders with circular cross sections. A set of boron nitride configurations can be generated by varying continuously the ratio of the radius of the two kinds of cylinders between 0 and 1. This class includes the triangular and graphite[21] structures previously studied as special cases. The Bravais lattice is hexagonal. With the choice of coordinate axis of Fig. 1, the primitive lattice vectors for the graphite and boron nitride structures are

$$\tau_1=\frac{a\sqrt{3}}{2}(1,\sqrt{3}), \tag{8a}$$

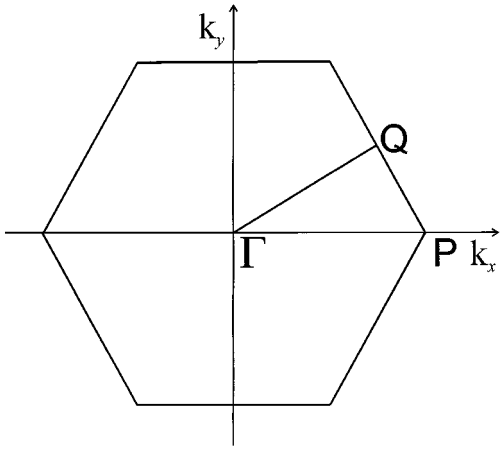

FIG. 2. Two-dimensional Brillouin zone for hexagonal lattice. The symmetry points P and Q are labeled using the Lommer notations (Ref. 22).

$$\tau_2=\frac{a\sqrt{3}}{2}(-1,\sqrt{3}). \tag{8b}$$

The unit cell contains two cylinders at the positions:

$$\mathbf{u}_1=-\mathbf{u}_2=a(0,1). \tag{9}$$

The nearest-neighbor distance for the graphite and BN structures is a. Because of the removal of one kind of cylinder in the triangular structure, it becomes $a\sqrt{3}$ in triangular configuration.

The primitive vectors of the reciprocal lattice are

$$\mathbf{h}_1=\frac{2\pi}{a\sqrt{3}}\left(1,\frac{1}{\sqrt{3}}\right), \tag{10a}$$

$$\mathbf{h}_2=\frac{2\pi}{a\sqrt{3}}\left(-1,\frac{1}{\sqrt{3}}\right). \tag{10b}$$

The first Brillouin zone turns out to be a hexagon as shown in Fig. 2 where the Lommer notations[22] are used to denote the symmetry points. The point group of the triangular and 2D graphite structure is D_{6h}. In the case of the 2D BN structure, the point group is D_{3h} because of the lack of the inversion operation.

To calculate the photonic band structures, we must first perform the Fourier transforms of $\eta(\mathbf{r})$ when the cylinders are filled with a material of dielectric constant ε_a and embedded in a background of dielectric constant ε_b. For structures with a unit cell including some cylinders of radius ρ_i centered at $\mathbf{u}_i$, the inverse of the dielectric constant is expressed as

$$\eta(\mathbf{r})=\varepsilon_b^{-1}+\sum_i\sum_{\mathbf{R}}\eta^{(i)}(\mathbf{r}-\mathbf{u}_i-\mathbf{R}), \tag{11}$$

where $\mathbf{R}$ denotes the translation vectors of the Bravais lattice and

$$\eta^{(i)}(\mathbf{r})=(\varepsilon_a^{-1}-\varepsilon_b^{-1})\,\theta(\rho_i-|\mathbf{r}|). \tag{12}$$

The Fourier transforms of $\eta(\mathbf{r})$ are

$$\eta(\mathbf{G})=\varepsilon_b^{-1}\delta_{\mathbf{G0}}+\sum_i\eta^{(i)}(\mathbf{G})e^{-i\mathbf{G}\cdot\mathbf{u}_i}. \tag{13}$$

For cylinders with circular cross sections, the Fourier transforms $\eta^{(i)}(\mathbf{G})$ only depend on $G=|\mathbf{G}|$. If the cylinders are not overlapping, we obtain

$$\eta^{(i)}(G)=(\varepsilon_a^{-1}-\varepsilon_b^{-1})\beta_i\frac{2J_1(G\rho_i)}{G\rho_i}, \tag{14}$$

where $\beta_i=\pi\rho_i^2/S_{\text{cell}}$ and $J_1(x)$ is the Bessel function of the first order. The graphite structure contains two identical cylinders located at $\mathbf{u}_1$ and $\mathbf{u}_2=-\mathbf{u}_1$. So, $\eta(\mathbf{G})$ can be expressed as

$$\eta(\mathbf{G})=\varepsilon_b^{-1}\delta_{\mathbf{G0}}+2\cos(\mathbf{G}\cdot\mathbf{u}_1)\,\eta^{(1)}(G), \tag{15}$$

whereas, by choosing the origin on the cylinder axis, we obtain for the triangular structure:

$$\eta(G)=\varepsilon_b^{-1}\delta_{G0}+\eta^{(1)}(G). \tag{16}$$

We define the filling factor β of these structures as the fraction of the cell area occupied by cylinders. These formulas underscore the effect of the arrangement and of the shape of the cylinders in the unit cell. Changes in the profile of the cross section modify $\eta^{(i)}(\mathbf{G})$, the presence of two cylinders in the unit cell acts on the structure factors by introducing modulation depending on reciprocal lattice vectors.

III. SYMMETRY ANALYSIS OF THE PHOTONIC STATES OF 2D HEXAGONAL BRAVAIS LATTICE

In this section, we investigate the opening of the gaps for two-dimensional hexagonal structures both of air cylinders in dielectric and also of dielectric cylinders in air from the symmetry properties. First, we are interested in the photonic states of the triangular structure. To classify the photonic states at the three high-symmetry points of the Brillouin zone, we must consider the irreducible representations of $\mathbf{k}$ group at the Γ, P, and Q points. The representations that are even (odd) under the inversion operation — if present — are labeled by the subscripts g (u) whereas the parity with respect to the reflection in the x-y plane, which is normal to the cylinders, is indicated by the superscripts $+$ or $-$. More information relative to the space groups concerned by this study are reported by Bassani and Pastori-Parravicini.[23] There are two sorts of polarization for the photonic states propagating in 2D lattices. The E polarization corresponds to states with the electric field parallel to the cylinders. So, the magnetic field lies in the lattice plane and is odd under the reflection in this plane and the corresponding Bloch states transform like the basis functions of the irreducible representations with superscript $-$. In the case of H polarization, the magnetic field is perpendicular to the lattice plane and invariant in the reflection. So, the photonic states are even and transform like the basis functions of the irreducible representations with superscript $+$.

Firstly, we examine the free-photon modes for the 2D hexagonal lattice following the lines well known in the study of the electronic band structures. The main difference lies in the dispersion relation that is linear for the photonic modes as opposed to the parabolic dispersion of free electrons.

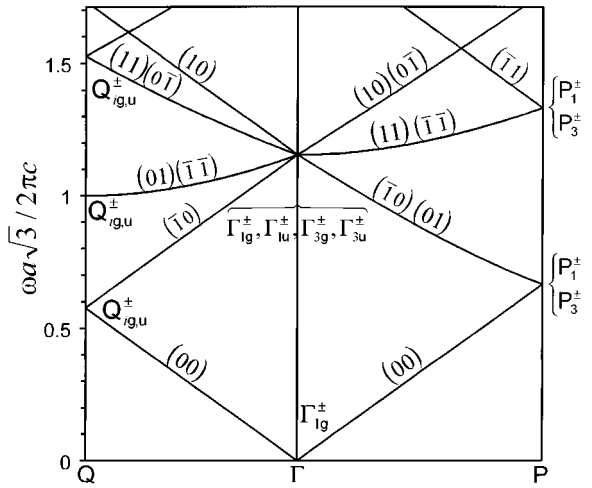

FIG. 3. Free-photon hexagonal bands. $(n_1 n_2)$ refers to plane waves with $\mathbf{G}=n_1\mathbf{h}_1+n_2\mathbf{h}_2$. $Q^{\pm}_{ig,u}$ means Q^{-}_{2g}, Q^{-}_{2u} for E polarization and Q^{+}_{1g}, Q^{+}_{1u} for H polarization.

Moreover, as the photonic states with E and H polarizations have the same frequency in the free-photon approximation, all the states are, at least, two-fold degenerate. The free-photon band structure for the 2D hexagonal lattice is plotted in Fig. 3 for the $\mathbf{k}$ vector belonging to the first Brillouin zone, along the two high-symmetry axes joining the Γ point to the P and Q points. The irreducible representations corresponding to each state are shown as well as the plane waves that contribute to this state. At Γ, a nondegenerate state $\Gamma^{\pm}_{1g}$ appears as well as a sixfold degenerate state consisting of two nondegenerate states $\Gamma^{\pm}_{1g}$, $\Gamma^{\pm}_{1u}$ and two two-degenerate states $\Gamma^{\pm}_{3g}$, $\Gamma^{\pm}_{3u}$. The states at the P point are due to the degeneracy between the nondegenerate state $P^{\pm}_1$ and the two-degenerate state $P^{\pm}_3$. To make a qualitative analysis of the formation of these gaps, we can research approximate solutions to Maxwell's equations by the perturbation theory, assuming that the spatial variations of the dielectric constant are small. Hereafter, we denote by E_i (H_i) the gap that occurs between the ith and $(i+1)$th bands for E (H) polarization.

A. *E* polarization

We will start to consider the E polarized photonic states of a hexagonal lattice and, first, we will study the opening of the gaps near the lowest free-photon modes at the P point. The threefold degeneracy existing in homogeneous materials would be split in two states, P^{-}_1 and P^{-}_3, with different energies. The symmetrized linear combinations of plane waves that transform like the rows of the irreducible representations are easily obtained from Ref. 23. As the same results hold for the P^{+} and P^{-} basis functions, we omit the superscript in their notation,

$$|\psi(P_1)\rangle=\frac{1}{\sqrt{3}}(|\mathbf{k}_P\rangle+|\mathbf{k}_P-\mathbf{h}_1\rangle+|\mathbf{k}_P+\mathbf{h}_2\rangle), \tag{17}$$

$$|\psi_1(P_3)\rangle=\frac{1}{\sqrt{6}}(2|\mathbf{k}_P\rangle-|\mathbf{k}_P-\mathbf{h}_1\rangle-|\mathbf{k}_P+\mathbf{h}_2\rangle), \tag{18}$$

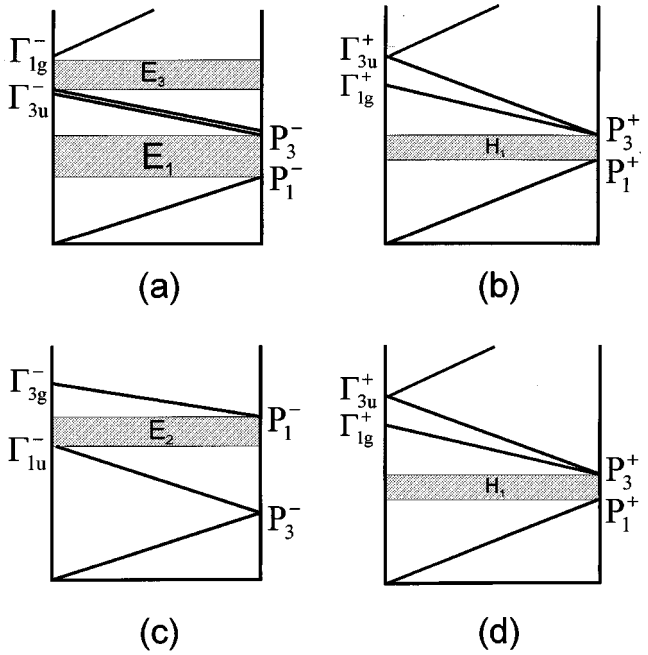

FIG. 4. Schematic representation of the opening of the gaps for 2D triangular structures of dielectric cylinders in air: (a) E polarization; (b) H polarization and for structures of air cylinders in dielectric material : (a) E polarization, (b) H polarization.

$$|\psi_2(P_3)\rangle=\frac{1}{\sqrt{2}}(|\mathbf{k}_P-\mathbf{h}_1\rangle-|\mathbf{k}_P+\mathbf{h}_2\rangle), \tag{19}$$

with $\mathbf{k}_P=(2\pi/a\sqrt{3})(2/3,0)$. In this basis, Eq. (6) is automatically diagonal. First, there is a nondegenerate state at

$$\omega_1^2=\langle\psi(P_1)|H|\psi(P_1)\rangle=c^2k_P^2(\eta_0+2\eta_1), \tag{20}$$

and a twofold degenerate state P^{-}_3 at

$$\omega_3^2=\langle\psi(P_3)|H|\psi(P_3)\rangle=c^2k_P^2(\eta_0-\eta_1), \tag{21}$$

where η_0 is the average of the inverse of the dielectric constant and η_1 holds for $\eta(|\mathbf{h}_1|)$. The splitting between the squared frequencies is equal to $3\eta_1$. For triangular structure consisting of cylinders with a dielectric constant ε_a, embedded in air, $\eta(G)$ has the opposite sign to $J_1(G\rho)$ and is thus negative for $G\rho<3.9$. On the contrary, in the case of air cylinders in a dielectric, $\eta(G)$ is positive in the same range. For nonoverlapping cylinders $\rho<a\sqrt{3}/2$ and $|\mathbf{h}_1|\rho<2\pi/\sqrt{3}$, which gives positive values for $J_1(G\rho)$. These results allow us to discuss the creation at the P point of a photonic band gap centered around $\omega^2=c^2k_P^2\eta_0$. For a 2D lattice of dielectric rods in air, the presence of a periodic dielectric constant leads to $P^{-}_1<P^{-}_3$. As the lowest state is nondegenerate, an E_1 gap opens between the first and second bands as can be seen in Fig. 4. Inversely, for lattices of circular voids in dielectric materials, $P^{-}_1>P^{-}_3$ and no gap appears at the P point. It is clear that an E_1 gap can only exist in triangular structures of dielectric rods in air with a difference between the squared frequencies equal to $3\eta_1$. The same qualitative estimations can be obtained for the photonic states at other points of the Brillouin zone. At the Γ point, the lowest photonic state with a nonzero frequency

is sixfold degenerate, consisting of two nondegenerate states Γ_{1g}^- and Γ_{1u}^- and of two nondegenerate states Γ_{3g}^- and Γ_{3u}^-. From the application of the first-order perturbation theory, we obtain

$$\omega_{1\varepsilon}^2=\langle\psi(\Gamma_{1\varepsilon})|H|\psi(\Gamma_{1\varepsilon})\rangle = c^2k_\Gamma^2[\eta_0+2\eta_2+\varepsilon(2\eta_1+\eta_3)], \tag{22a}$$

$$\omega_{3\varepsilon}^2=\langle\psi(\Gamma_{3\varepsilon})|H|\psi(\Gamma_{3\varepsilon})\rangle = c^2k_\Gamma^2[\eta_0-\eta_2-\varepsilon(\eta_1-\eta_3)], \tag{22b}$$

where $k_\Gamma^2=(2\pi/a\sqrt{3})^2(4/3)^2$, $\eta_2=\eta(|\mathbf{h}_1-\mathbf{h}_2|)$, and $\eta_3=\eta(|2\mathbf{h}_1|)$. ε equals 1 or -1 according to whether the irreducible representations are even (g) or odd (u) with respect to the inversion operation. For dielectric rods in air, at small filling factors, the photonic state Γ_{1g}^-, which has the characteristics of a bonding state, is the lowest-frequency state, because all the η contributions are negative and add to each other. The photonic states Γ_{1g}^- and Γ_{1u}^- are expected to be widely separated in frequency. The position of the other states is rather sensitive to the characteristics of the band-gap material and mainly depends on the radius of the cylinders, because, for large filling factors β, $\eta(G)$, which varies as $J_1(G\rho)$, changes its sign for $G\rho=3.9$. The difference between the squared frequencies of the states Γ_{1g}^- and Γ_{1u}^- calculated from Eq. (22) is

$$\omega_{3u}^2-\omega_{1g}^2=-c^2k_\Gamma^2(\eta_1+3\eta_2+2\eta_3). \tag{23}$$

For small β values, all the η contributions are negative and Γ_{3u}^- is above Γ_{1g}^-. The largest contribution to Eq. (23) is due to η_2 and η_3 terms that become positive for β larger than about 0.35 whereas η_1 always remains negative. So, the difference between the squared frequencies changes its sign and causes a crossing of the two states Γ_{1g}^- and Γ_{1u}^-. Therefore, we can predict the sequence of the states $\Gamma_{1g}^-<\Gamma_{3u}^-$, $\Gamma_{3g}^-<\Gamma_{1u}^-$ for low filling factors and the sequence $\Gamma_{3u}^-<\Gamma_{3g}^-\approx\Gamma_{1g}^-<\Gamma_{1u}^-$ for larger β values. In this case, there is the opening of an E_3 gap between the third and fourth bands. Consider now the case of air cylinders in a dielectric material. For the same geometry, the Fourier transforms $\eta(G)$ have the opposite sign to those of a lattice of dielectric cylinders in air. The order of the states is reversed giving, at low filling levels, the sequence $\Gamma_{1u}^-<\Gamma_{3g}^-$, $\Gamma_{3u}^-<\Gamma_{1g}^-$. However, the order of the two states depends on the β values. The difference between the squared frequencies is

$$\omega_{3g}^2-\omega_{1u}^2=c^2k_\Gamma^2(\eta_1-3\eta_2+2\eta_3). \tag{24}$$

In this case, the contributions of η_2 and η_3 are opposite and η_1 determines the sign of the difference. We expect the sequence $\Gamma_{1u}^-<\Gamma_{3g}^-$ for the lowest states, which leads to the opening of an E_2 gap between the second and third bands. Similar analysis can be made at the Q point for which the free-photon states are twofold degenerate. The periodic variation of the dielectric constant splits these states between two nondegenerate states Q_{2g}^- and Q_{2u}^- separated by $2\eta_1$ whatever the nature of the cylinder and of the background. We can now describe the formation of the photonic band gaps on the whole of the Brillouin zone for the E polarization in 2D triangular structures of cylinders. In the case of air cylinders in a dielectric, an E_2 gap can be opened. For dielectric cylinders embedded in air, there is an E_1 gap and, for not too small β values, another E_3 gap appears.

B. *H* polarization

A similar study can be carried out in order to estimate the gap opening for the H polarization. The differences between the two polarizations are due to the modifications of the matrix to be diagonalized. In the H polarization, the matrix elements depend on the scalar product $(\mathbf{k}+\mathbf{G})\cdot(\mathbf{k}+\mathbf{G}')$ [see Eq. (7)] whereas in E polarization, this is the product of the modulus that is to be considered. At the P point, there are three equivalent vectors that contribute to the lowest-frequency state and the angles between them are equal to $2\pi/3$. So, the scalar product is obtained by multiplying the product of the modulus by $-1/2$. With respect to the E polarization, the inversion of the P_1 and P_3 states occurs, and there is a reduction by half of the gap width. Considering, for instance, a 2D lattice of dielectric cylinders in air, the P_3^+ state lies under the P_1^+ state. In fact, this situation only exists for small β values because the splitting is much smaller than for the E polarization. The influence of plane waves with larger wave vectors can be estimated in the framework of the perturbation theory. Considering the contribution due to the first upper band, we obtain

$$\delta(\omega_1^2)=-c^2k_P^2\frac{4(\eta_1-\eta_2)^2}{3\eta_0} \quad \text{with } \omega_1^2=c^2k_P^2(\eta_0-\eta_1), \tag{25a}$$

$$\delta(\omega_3^2)=-c^2k_P^2\frac{(\eta_1+2\eta_2)^2}{3\eta_0} \quad \text{with } \omega_3^2=c^2k_P^2\left(\eta_0+\frac{\eta_1}{2}\right). \tag{25b}$$

At low filling factors, for a lattice of dielectric cylinders in air, η_1 and η_2 are negative and $\delta(\omega_1^2)$ is small because of the cancellation of the two contributions. The P_1^+ state is slightly repelled by the nearest upper state in comparison with the P_3^+ state, which remains the lowest-lying state. For larger β values, η_2 becomes positive. The two contributions η_1 and η_2 add up for $\delta(\omega_1^2)$, whereas they cancel each other out for $\delta(\omega_3^2)$. In this case, the P_1^+ state is strongly repelled by the upper state and lies lower than the P_3^+ state. For lattices of air cylinders in dielectric material, the states at the P point are obtained from Eq. (25). In this case, the Fourier transforms $\eta(G)$ are positive. P_1^+ is lower than P_3^+ and the sequence is not affected by increasing the filling factor because the repulsive effect of the upper bands is not dependent on the sign of $\eta(G)$ and repels P_1^+ more than P_3^+. At the Γ point, the situation is more complicated because the lowest state is formed by six equivalent plane waves. At the first order of the perturbation theory, the squared frequencies are

$$\omega_{1\varepsilon}^2=c^2k_\Gamma^2[\eta_0-\eta_2+\varepsilon(\eta_1-\eta_3)], \tag{26a}$$

$$\omega_{3\varepsilon}^2=c^2k_\Gamma^2\left[\eta_0+\frac{\eta_2}{2}-\varepsilon\left(\frac{\eta_1}{2}+\eta_3\right)\right]. \tag{26b}$$

In the case of dielectric cylinders in air, all the $\eta(G)$ are negative at low filling levels and Γ_{3u}^{+} is the lowest state. The difference between the squared frequency of this state with its nearest-neighbor Γ_{1g}^{+} is given by

$$\omega_{3u}^2-\omega_{1g}^2=c^2k_\Gamma^2(\eta_1-3\eta_2-4\eta_3), \tag{27}$$

which is of the same type as Eq. (23). By the same analysis as for the E polarization, we conclude that increasing the filling factor changes the sign of the dominant contribution due to η_2 and η_3. The difference becomes positive and the sequence $\Gamma_{1g}^{+}<\Gamma_{3u}^{+}$ is expected. Consequently, considering lattices of dielectric cylinders in air, the lowest states are P_1^{+} and Γ_{1g}^{+} and we expect the opening of the H_1 gap. For lattices of air cylinders in dielectric material, we deduce from Eq. (26) the sequence $\Gamma_{1u}^{+}<\Gamma_{3g}^{+}<\Gamma_{3u}^{+}<\Gamma_{1g}^{+}$ at low filling levels. To see the β dependence of the position of these states, we calculate

$$\omega_{3g}^2-\omega_{1u}^2=\tfrac{1}{2}c^2k_\Gamma^2(\eta_1+2\eta_2-2\eta_3). \tag{28}$$

The η_2 and η_3 contributions cancel each other out. The difference is positive because it has the sign of η_1. Therefore, we expect in the case of air cylinders the sequence $\Gamma_{1u}^{+}<\Gamma_{3g}^{+}$ for various filling levels. As the degeneracies of the free-photon bands at the Q point are always lifted, the H_1 gap can occur for this configuration.

We wish to draw some general rules from this study of the 2D triangular structure of cylinders embedded in a background with a different dielectric constant for not too small filling factors. First, for the E polarization, the opening of the gap varies according to whether the dielectric constant of the cylinders is larger or smaller than that of the background. For hole cylinders in dielectric material, only the E_2 gap can occur at low frequencies whereas the two gaps E_1 and E_3 can exist for dielectric cylinders in air. However, on the other hand, for the H polarization, the opening of the gap does not depend on the nature of the cylinders and the H_1 gap is present in both cases. All these results are confirmed by the numerical calculations carried out on 2D triangular structures.[14–17] Comparison with the results of our analysis shows that our predictions on the opening of the gap remain valid on a large range of filling factors. Our quantitative analysis of photonic band gaps by a perturbative approach from the free-photon bands gives a good account of the basic properties of the 2D hexagonal lattices and should make the research of optimized structures easier.

As the point group of the triangular and graphite structures is the same (D_{6h}), similar analysis can be carried out for the graphite structure, provided that the modifications of the Fourier transforms of the dielectric constant due to the structure factors are taken into account. For the first star of the $\mathbf{G}$ vectors formed by the set of vectors generated from the $\mathbf{h}_1$, the structure factor is -1, for the second and the third stars, it is respectively equal to 2 and -1. As the splitting of the lowest P state only depends on η_1 as seen above, the results obtained for the triangular structure can be applied to the graphite structure by only changing the sign of the η_1 contribution. It follows that the order of the P_1 and P_3 states is opposite in both structures. For instance, in the case of E polarization, the E_1 gap, which exists at the P point for a triangular arrangement of air cylinder in dielectric, must disappear when going to the graphite structure by removing the cylinders at the hexagon centers. The analysis of the opening of gaps can be carried out at other symmetry points and for the H polarization along the same lines as for the triangular structure.

Also, in the BN structure, one can make predictions on the sequence of photonic states. Since the inversion is not present in the point group (D_{3h}), the even and odd irreducible representations coincide at the Γ and Q points. On the other hand, the representations for the P point are not related simply to those at the P point of graphite. The most striking difference between the two structures lies in the fact that there is no two-dimensional irreducible representations in BN so that the degeneracy is completely lifted, always leading to the existence of gaps at the zone edges. It can be expected that there are more openings of gaps in the boron nitride structure than in the triangular and graphite ones for which the symmetry induces degeneracies.

IV. PHOTONIC BAND GAPS

To optimize the structures in order to maximize the width of the absolute PBG's, we have considered a whole class of BN structures consisting of two hexagonal sublattices made up of parallel cylinders of the same material with different radii ρ_1 and ρ_2. These structures can be characterized by two parameters, the filling factor β and the radius ratio $\alpha=\rho_1/\rho_2$. Note that this set includes the triangular structure for $\alpha=0$ and the graphite one for $\alpha=1$. We have studied the evolution of PBG's as functions of α for β given values, which allows the description of structures with the same average dielectric constant $\varepsilon_{\mathrm{av}}$. Configurations with different filling factors have been examined and we present here the most significant results. As we only consider here the case of nonoverlapping cylinders, the maximum filling factor for the graphite structure $\beta=60\%$ is reached when the cylinder diameter is equal to the distance between two nearest-neighbor cylinders. This is smaller than for the triangular case because the cylinders at the hexagon centers have been removed. We examine the two following complementary configurations. The first one consists of air cylinders ($\varepsilon_a=1$) in GaAs ($\varepsilon_b=13.6$). The second one is formed by cylinders of GaAs in air. GaAs has been chosen because it presents interesting optical properties in the infrared domain and is representative of many semiconductors. This limitation is not essential and calculations on other systems of the same nature give similar results. We use 475 plane waves in the calculations, which ensures sufficient convergence for the frequencies of interest for the studied structures.

We first consider the BN structure of air cylinders in GaAs at $\beta=60\%$, which corresponds to the graphite close-packed configuration. We show in Fig. 5, the evolution of PBG's with respect to the radius ratio. Many gaps appear for E polarization, their number varying according to the α values. As predicted by symmetry analysis, an E_1 gap that cannot exist in the triangular structure opens up for $\alpha>0$ and reaches its maximum width for the graphite structure at $\alpha=1$. The E_2 gap evolves in a complementary way. It is maximum for $\alpha=0$ and closes over 0.1. New gaps due to the lower symmetry of the BN structure appear only at interme-

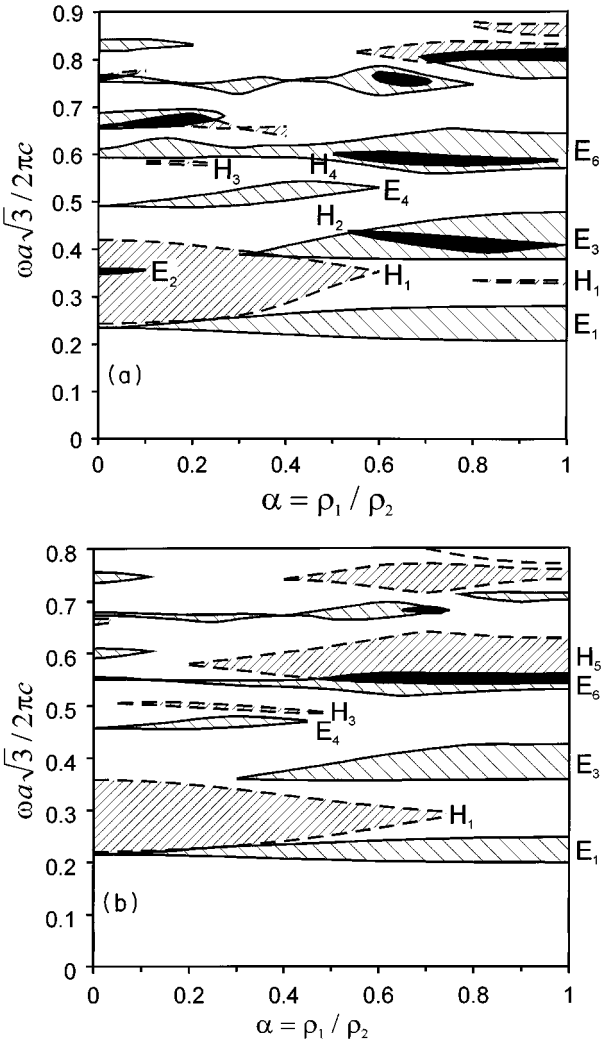

FIG. 5. Photonic band gaps for E polarization (solid line) and H polarization (dashed line) of boron nitride structures of air cylinders in GaAs for (a) $\beta=60\%$, and (b) $\beta=50\%$. The absolute band gaps are represented in black.

diate values of α. For H polarization, only one H_1 gap occurs in the triangular structure. Its width decreases for an increasing value of α. This gap closes for $\alpha=0.6$ and opens again for $0.8<\alpha<1$. Some other gaps only lie in the intermediate range of α and do not exist at the two higher-symmetry limit structures. There are three absolute PBG's in this configuration. The first one is due to the overlap of E_2 and H_1 gaps and its greater width is obtained for the triangular configuration. Its existence has been previously reported by some other authors.[14–17] Two other gaps E_3-H_2 and E_6-H_4 occur for $0.5<\alpha<1$. They are characteristic of BN structure and their maximum widths are 7% and 4%, respectively. Figure 6 shows the photonic band structure of the BN structure for $\beta=60\%$ and $\alpha=0.8$, which is the configuration giving the E_3-H_2 gap maximum. This structure is not very different from the triangular one for the same filling factor apart from the appearance of many gaps at the P point, whatever the polarization may be. This effect is due to the lack of the inversion operation and can be analyzed within the perturbation theory. The BN structure with an average dielectric constant $\varepsilon_{\mathrm{av}}$ can be seen as a triangular structure

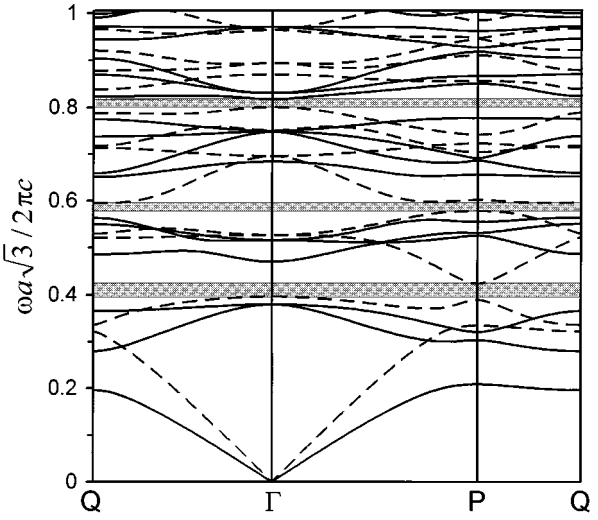

FIG. 6. Photonic band structure for E polarization (solid line) and H polarization (dashed line) of boron nitride structure of air cylinders in GaAs for $\beta=60\%$, $\alpha=0.8$.

with $\varepsilon'_{\mathrm{av}}=(2/3)\varepsilon_{\mathrm{av}}$, perturbed by an antisymmetric contribution depending on α. Symmetry considerations show that only the two-dimensional P_3 states at the zone edges are perturbated at the first order. This allows us to understand qualitatively the opening of gaps at the P point whereas the overall behavior of the photonic band structure is hardly affected. At $\beta=60\%$, the cylinders are in the close-packed configuration and these structures will be probably rather difficult to realize because the dielectric layers between the cylinders are very thin. We have investigated the evolution of the PBG's for a smaller value of the filling factor $\beta=50\%$. Comparison between Fig. 5(a) and 5(b) shows that gap widths strongly depend on the filling factor. All the gaps shrink and the narrowest ones like E_2, H_2, and H_4 are suppressed. So, absolute PBG's will be only observed for large filling factors. Consequently, the most promising hexagonal structure of air cylinders in GaAs is the triangular one for which the absolute band gap E_2-H_1 can be widened by increasing the filling factor up to 0.91. In fact, to keep sufficiently rather thick layers between the cylinders, β must be limited to 70%.

We have also examined the case of BN structures formed by GaAs rods in air. In Fig. 7, we present the dependence of PBG's on the radius ratio for $\beta=30\%$. This value has been chosen because it is in this vicinity that the absolute band gaps are the largest. For E polarization, E_1 and E_3 gaps close when going from triangular to graphite structure whereas the E_2 gap opens up. This confirms the correctness of symmetry analysis, which predicts at once an opposite variation of the widths of the E_1 and E_2 gaps versus α for a given configuration, as well as of the width of the E_1 gap for two complementary structures like air cylinders in GaAs and GaAs rods in air. Large E_4 and E_7 gaps occur for the intermediate values of α and close near the two limit values. Some gaps also appear for H polarization. The lowest-frequency gap H_1 shrinks for increasing α values and closes above $\alpha=0.7$. The H_2 gap only exists for BN structures with $0.1<\alpha<0.7$. More interesting is the appearance of H_3 and H_5 gaps above $\alpha=0.7$. These gaps widen when α increases.

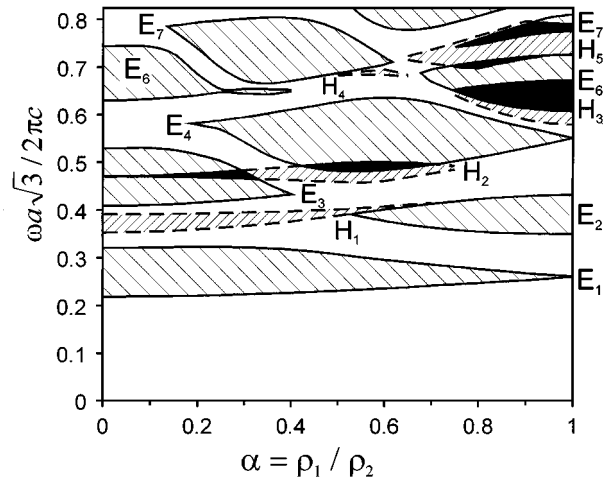

FIG. 7. Photonic band gaps for boron nitride structure of GaAs cylinders in air for $\beta=30\%$.

The E_3-H_2 gap exists for $0.1<\alpha<0.4$; however, its width remains small. The most important result is the appearance of two absolute band gaps E_6-H_3 and E_7-H_5, which are not present in triangular structure of GaAs rods in air.[17] As their widths are maximum for $\alpha=1$, the graphite structure appears as the most interesting configuration to get optimal absolute band gaps for lattices of GaAs rods in air. The dispersion of the low-frequency photonic bands of the graphite structure[21] presents some similarities with those of triangular structures of air cylinders in GaAs.[19] Results for E polarization have the same features. In particular, the sequence of the lowest-frequency states and the opening of the gaps are the same. More differences exist for H polarization because of the smallness of the gaps. In the triangular structure, there is only a H_1 gap due to the splitting at the P point, whereas for the graphite structure, this gap has disappeared and two other gaps H_3 and H_5 open. This resemblance can be easily understood from the geometric disposition of the cylinders in the graphite structure. For close-packed arrangement, this configuration is equivalent to a triangular structure with the lattice constant $a\sqrt{3}$ formed by air cylinders with a noncircular section. The lowest gap E_6-H_3 is centered at $\omega a/2\pi c=0.37$ for $\beta=30\%$ with a 10% relative width. This can be compared with PBG's obtained for an optimized triangular structure of hole cylinders in GaAs.[17] Taking into account the fabrication limits, the largest absolute PBG attainable in this case is centered at $\omega a/2\pi c\approx 0.4$ for $\beta\approx 70\%$ (where here a is the lattice parameter). As for a lattice of air cylinders in GaAs, the proportion of material is equal to $1-\beta$; it can be seen that this proportion is the same as for the two considered structures that have consequently the same average dielectric constant. For such a graphite structure, PBG's can be centered in the near infrared. For instance, a graphite structure formed by GaAs rods with 0.24-μm diameter separated by a distance $a=0.50$ μm gives an absolute PBG centered at $\lambda=0.9$ μm. A second absolute band gap of the same width is obtained for $\omega a/2\pi c=0.55$ at $\beta=15\%$ by the superposition of E_7 and H_5 gaps. It will be centered on the same wavelength for a lattice with rods of the same diameter separated by the distance $a=0.34$ μm. In these two structures, the diameter of the rods is large and the realization of these lattices does not require etching of thin dielectric layers. The appearance of these gaps is essential and shows that the graphite structure of dielectric rods has good potential for the realization of photonic-band-gap materials.

V. CONCLUSION

We have presented in this paper a class of two-dimensional photonic crystals based on the 2D hexagonal lattice. These structures consist of parallel cylindrical rods whose axis forms a two-dimensional arrangement of hexagons. By a perturbation approach using symmetry arguments, we have drawn some general rules on the sequence of the photonic states at the high-symmetry points and we have been able to study the gap opening according to whether the dielectric constant of the cylinders is larger or smaller than that of the background. The photonic band structure and the numerous gaps occurring in these systems have been calculated as functions of the cylinder diameter. We show that absolute band gaps are obtained for large variation ranges. Among these hexagonal structures, the largest absolute band gaps appear for triangular structures of cylindrical holes in dielectric as well as for graphite structures of dielectric rods in air.

ACKNOWLEDGMENTS

The Groupe d'Etude des Semiconducteurs is ''Unité de Recherche Associée au Centre National de la Recherche Scientifique No. 357.'' We thank the ''Centre National Universitaire Sud de Calcul de Montpellier'' for an allowance of computer time.

[1] E. Yablonovitch, Phys. Rev. Lett. **58**, 2059 (1987).
[2] S. John, Phys. Rev. Lett. **58**, 2486 (1987).
[3] E. Yablonovitch and T. J. Gmitter, Phys. Rev. Lett. **63**, 1950 (1989).
[4] S. Satpathy, Ze Zhang, and M. R. Salehpour, Phys. Rev. Lett. **64**, 1240 (1990).
[5] K. M. Leung and Y. F. Liu, Phys. Rev. Lett. **65**, 2646 (1989).
[6] Ze Zhang and S. Satpathy, Phys. Rev. Lett. **65**, 2650 (1990).
[7] K. M. Ho, C. T. Chan, and C. M. Soukoulis, Phys. Rev. Lett. **65**, 3152 (1990).
[8] E. Yablonovitch, T. J. Gmitter, and K. M. Leung, Phys. Rev. Lett. **67**, 2295 (1991).
[9] For recent reviews, see the articles in *Photonic Bandgaps and Localization*, edited by C. Soukoulis (Plenum, New York, 1993) and in the special issue of J. Opt. Soc. Am. B **10** (1993), edited by C. M. Bowden, J. P. Dowling, and H. O. Everitt.
[10] P. R. Villeneuve and M. Piché, Prog. Quantum Electron. **18**, 153 (1994)
[11] J. D. Joannopoulos, R. D. Meade, and J. N. Winn, in *Photonic*

Crystals, Molding the Flow of Light (Princeton University Press, Princeton, 1995).
[12] E. Özbay, E. Michel, G. Tutte, R. Biswas, M. Sigalas, and K. M. Ho, Appl. Phys. Lett. **64**, 2059 (1994).
[13] Shanhui Fan, P. R. Villeneuve, R. D. Meade, and J. D. Joannopoulos, Appl. Phys. Lett. **65**, 1466 (1994).
[14] M. Plihal and A. A. Maradudin, Phys. Rev. B **44**, 8565 (1991).
[15] R. D. Meade, K. D. Brommer, A. M. Rappe, and J. D. Joannopoulos, Appl. Phys. Lett. **61**, 495 (1992).
[16] P. R. Villeneuve and M. Piché, Phys. Rev. B **46**, 4969 (1992).
[17] R. Padjen, J. M. Gérard, and J. Y. Marzin, J. Mod. Opt. **41**, 295 (1994).
[18] P. L. Gourley, J. R. Wendt, G. A. Vawter, T. M. Brennan, and B. E. Hammons, Appl. Phys. Lett. **64**, 687 (1994).
[19] J. M. Gérard, A. Izraël, J. Y. Marzin, R. Padjen, and F. R. Ladan, Solid-State Electron., **37**, 1341 (1994).
[20] K. Inoue, M. Wada, K. Sakoda, A. Yamanaka, M. Hayashi, and J. W. Hus, Jpn. J. Appl. Phys. **33**, L1463 (1994).
[21] D. Cassagne, C. Jouanin, and D. Bertho, Phys. Rev. B **52**, R2217 (1995).
[22] W. M. Lommer, Proc. R. Soc. London A **227**, 330 (1955).
[23] F. Bassani and G. Pastori-Parravicini, in *Electronic States and Optical Transitions in Solids* (Pergamon, Oxford, 1975).